Artificial Intelligence for Detection of Lung Cancer using Transfer Learning and Morphological Features

Nafe Muhtasim[1†], Umma Hany[2*†], Tahmina Islam[3], Nusrat Nawreen[4] and Abdullah Al Mamun[5]

[1,2,3,4,5]Department of Electrical and Electronic Engineering, Ahsanullah University of Science and Technology, Dhaka, Bangladesh.

*Corresponding author(s). E-mail(s): uhany.eee@aust.edu;
Contributing authors: nafemuhtasim98@gmail.com; tahminaislam837@gmail.com; nahinnawreen@gmail.com; abdullah.m.eee@hotmail.com;
†These authors contributed equally to this work.

Abstract

Lung cancer is an uncontrolled growth of tissue causing a lump in the human lung. If lung cancer can be detected early, it can increase the survival rate. Therefore, a multi-classification approach of lung tumor detection with high computational effectiveness is required. In this paper, a multi-classification approach of Lung tumor detection and classification is proposed using artificial intelligence on Computed Tomography (CT) scan images. Different pre-processing steps are applied for resizing, smoothing, and enhancement of the CT images. Then, two different approaches for feature extraction using VGG16 transfer learning (TL) and morphological segmentation are proposed. Morphological segmentation and feature extraction are applied for the segmentation of the region of interest and to extract the distinct features. Finally, the proposed deep learning architecture and seven different machine learning algorithms are applied on the preprocessed data and the extracted features for the classification of lung tumors into three classes; malignant, benign and normal. It is observed that all the ML algorithms perform with reasonably high accuracy using the low dimensional morphological features. It is observed from the 5-fold cross-validation results that logistic regression (LR) performs with 99.36% accuracy in 23.71 sec time using the preprocessed data. Whereas, using the morphological features, k-Nearest Neighbor (KNN) and the Support Vector Machine (SVM) perform with the highest accuracy of 99.76% with very reduced computational time of 0.017 sec and 0.008 sec, respectively.

Keywords: Lung cancer recognition, Transfer learning, Morphological feature extraction

1 Introduction

Lung cancer is a malignant tumor. People accompanying pleura disease, like emphysema and premature chest problems, have more chance to be diagnosed with body part malignancy. Overuse of tobacco, cigarettes, and secondhand smoke is the major risk factor that leads to bronchi malignancy. The size of the tumor and the extent of its spreading determines the stage of the tumor[1]. Lung Tumors can be classified into two types; Benign and Malignant. A tumor that is no threat to invading other tissues is considered Benign. When the cell is abnormal and can grow uncontrollably

and spread to other parts of the body, is a cancerous or Malignant tumor. This spreading process is called metastasis [2]. Lung disease can be seen on chest radiographs and computed tomography (CT) scan images. Among these, CT scan images are the most reliable and effective method as it shows a detailed picture of the object and its growth [3]. In the literature, there are several works on image segmentation, feature extraction, detection, and classification of lung cancer [4].

In [5], the authors propose various machine learning methods for detecting lung cancer nodules from CT scan images and report 82.43% accuracy using Artificial Neural Network (ANN) with image processing and 93.24% accuracy using Decision tree without image processing. However in [5], noise removal methods are not applied before using the image set, and the whole chest radiograph is used as the input for machine learning methods. The authors in [6] propose lung cancer detection in Positron Emission Tomography/Computed Tomography (PET/CT) images by using 3 texture features and 10 fractal feature descriptors classified by machine learning and artificial intelligence techniques. The authors report 98.10% accuracy in [6] using Support Vector Machine (SVM) with Radial Basis Function (RBF) kernel for binary classification of the lung tumors. In the paper [7], high dimensional feature extraction using DenseNet and non-negative sparse and collaborative representation (NSCR) binary classification of benign and malignant lung tumors are proposed to obtain 99.10% accuracy in 3234.63 sec training time. The authors in [8] evaluate several available machine-learning algorithms in the literature that can be used for lung cancer detection associated with IoT devices. The authors in [9] propose a parallel deep learning model with a hybrid attention mechanism for image segmentation of lung tumors applying DenseNet module and report 94.61% segmentation accuracy. In [10], the segmented images of non-small cell lung cancer (NSCLC) are fed into a hybrid feature detection and extraction model called Maximally Stable Extremal Regions and Speeded Up Robust Features (MSER-SURF). Then, the thirty-three (33) MSER-SURF features are extracted and classified to detect NSCLC tumor using the 1D CNN model. The reported classification accuracy in [10] is 96 $\pm$ 3%. In [11], machine learning algorithms such as the Multi-layer Perceptron (MLP), K-Nearest Neighbor (KNN), and SVM classifier are used to classify lung diseases using the Gray Level Co-occurrence Matrix (GLCM) including eight (08) features. The reported accuracy using MLP, SVM and KNN is 98%, 70.45% and 99.2%, respectively using 400 lung disease CT scan images. The authors in [12] compare the accuracy of lung cancer classification of SVM, KNN, and Convolutional Neural Network(CNN) by WEKA tool at the beginning phase of malignancy. The resulting outcome shows that SVM gives the outcome with 95.56%, CNN with 92.11%, and KNN with 88.40%. In [13], the authors propose an ingenious methodology of lung tumor detection using image segmentation for feature extraction and machine learning-based classification to classify the test images of lung tumors into normal and abnormal. In the paper [14], the author classifies lung cancer images into two classes (benign and malignant) using fuzzy logic accompanied by region of interest (ROI) extraction. SURF technique and Genetic algorithm (GA) are used for feature extraction and optimization in [14] and then SVM with Feed-Forward Back Propagation Neural Network (FFBPNN) is used to create a hybrid classification algorithm reducing the computational complexity. The authors report an overall classification accuracy of 98.08% in [14]. The authors in [15] propose the methods of lung cancer detection and prediction using different image processing, filter-based feature extraction techniques, and SVM classifiers. In [15], the authors use 110 test cases from the IQ-OTHNCCD lung cancer dataset [16] to classify them into three classes; normal, benign or malignant and reported 89.88% classification accuracy. The authors in [17] use CNN and Google Net deep learning algorithms for lung cancer detection and binary classification and achieve a precision of 98% in detection and classification.

Though there are several works in the literature, most of the works are on binary classification of lung tumors or predicting a specific type of cancer without applying cross-validation. Additionally, the computational time has not been reported in most of the above works. Hence, a multi-classification approach with high computational effectiveness is required for the fast detection and classification of lung tumors. In this paper, we propose a multi-classification approach for lung tumor detection and classification as normal, benign, and malignant with high computational effectiveness by applying machine learning and deep learning methods on the CT scan images. We use the IQ-OTHNCCD lung cancer dataset [16] collected from the Kaggle [18]. The dataset contains a

total of 1190 CT scan images of three classes; normal, benign, and malignant. First, we apply preprocessing steps to resize and enhance the images. Then, the preprocessed raw data are applied to the classifiers. However, as the raw data requires high processing time, we apply the VGG16 model for transfer learning (TL) based feature extraction. The extracted TL features are then applied to the classification to reduce the processing time. For real-time health care and improved computational intelligence, we propose morphological feature extraction by applying image segmentation of the region of interest (ROI) of different types of lung tumors using thresholding and morphological operations. Then, distinct features of the segmented ROI of the tumors are extracted and applied for classification. Morphological feature extraction reduces the dimensionality of the data significantly resulting in low computational complexity and processing time increasing the computational intelligence of the proposed systems. We apply different deep learning and machine learning-based classifiers to train the images and to classify the tumors into three labels; normal, benign, and malignant. Among the classifiers, the deep learning-based convolutional neural network (CNN) shows 98.64% accuracy with preprocessed raw data. Among the machine learning classifiers, logistic regression (LR) shows 100% accuracy using both preprocessed raw data and transfer learning features. Whereas, using the extracted morphological features, all the machine learning algorithms perform with significantly high accuracy in comparatively lower computational time. Among them KNN and SVM show the highest accuracy with the least computational time. We apply 5-fold cross-validation to mitigate the overfitting problems and to verify the best possible accuracy using the LR, KNN, and SVM algorithms. It is observed from the results that LR performs with 99.36% and 99.27% accuracy with preprocessed data and TL features in 23.71 sec and 16.51 sec computational time, respectively. Whereas, both KNN and SVM perform with 99.76% accuracy in 0.017 sec and 0.008 sec time, respectively. Thus, it may be concluded that using the low dimensional morphological features, KNN and SVM classification algorithms perform the best in the least computational time. The accuracy is also compared to other methods in the literature and it is found that the proposed methods outperform the literature in terms of accuracy and computational time.

2 System overview

The system flow of the lung tumor detection and classification using CT scan images is shown in Figure 1. The system starts with lung image acquisition using a CT scanner. The collected CT scan images are loaded into the system for preprocessing. We propose two methods of data preprocessing using Scaling and normalization and by using Data cropping and enhancement. The processed images are forwarded to the feature extraction modules. The extracted features of the processed data are then trained and tested by the classification modules to predict the class of lung tumors. Lung tumors are classified both by using machine learning and deep learning methods. In our proposed approach as shown in Figure 1, we classify the lung tumors using three approaches to compare the accuracy of classification. In the first approach, the classifier receives the preprocessed raw data for classification using machine learning and deep learning methods. In the second approach, the features of the preprocessed data are extracted using VGG16-based transfer learning and classified using machine learning or deep learning methods. In the third approach, the preprocessed data are applied to the morphological segmentation and feature extraction methods to reduce the dimensionality of data and the processing time, and then the extracted features are applied to the classifier for classification of the lung tumors. Using the three approaches, the CT scan images of the lung tumors are classified into three classes Benign, Malignant or Normal. The predicted label or class of the lung tumors is then compared to the original label to verify the accuracy. The detailed methodologies are explained in the following section.

3 Data Preprocessing

We apply different preprocessing methods on the collected datasets. The data source and the preprocessing methods are explained below.

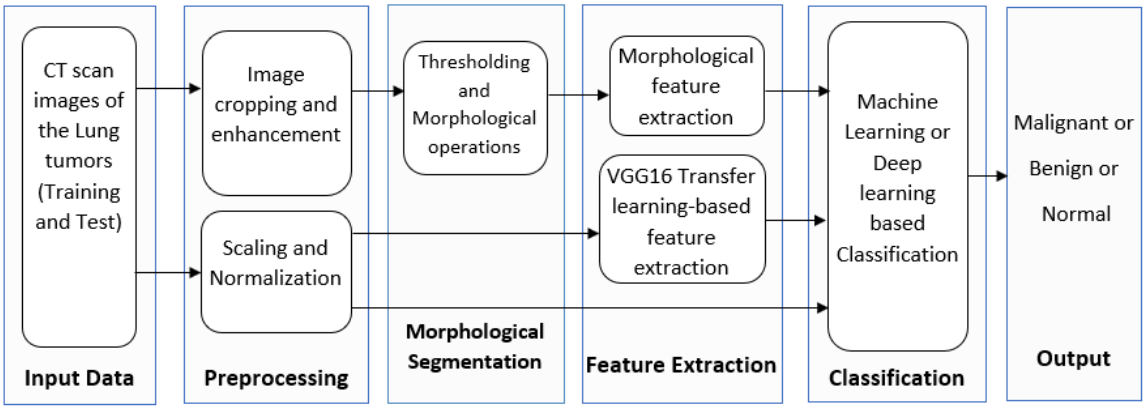

Fig. 1 System overview

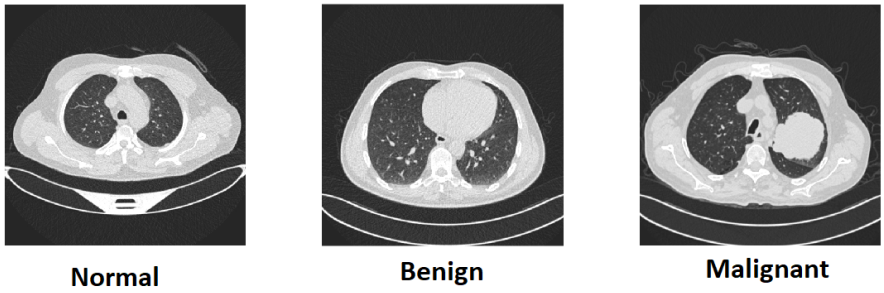

Fig. 2 CT scan images of lung tumors of three classes

3.1 Data source

We use the IQ-OTHNCCD lung cancer dataset [16] from Kaggle [18]. The IQ-OTHNCCD lung cancer dataset is collected at Iraq-Oncology Teaching Hospital or National Center for Cancer Diseases (IQ-OTH/NCCD) and marked by the oncologists and radiologists. The dataset contains a total of 1190 images representing CT scan slices of 110 cases. These cases are grouped into three classes: normal, benign, and malignant, of these, 40 cases are diagnosed as malignant; 15 cases are diagnosed as benign; and 55 cases are classified as normal cases. The 110 cases vary in gender, age, educational attainment, area of residence, and living status. The amount of data is increased by collecting data from a single case with different sides and angles during data acquisition. Each scan contains several slices ranging from 80 to 200 slices, each representing an image of the human chest with different sides and angles.

3.2 Preprocessing

The collected dataset contains CT scan images of normal, benign, and malignant type lung tumors. Figure 2 shows the samples of three classes of lung tumors. First, we split the dataset of CT images into training and test images. 80% of the data are used for training and 20% are used for testing. Then, the CT scan images are preprocessed using two methods. The first method is used to preprocess the datasets before applying them to transfer learning, machine learning, and deep learning models. The second method of preprocessing is applied only before morphological feature extraction. The methods are explained as follows.

3.2.1 Scaling and normalization

The data is preprocessed using scaling and normalization. In this preprocessing, the CT scan data in jpg format are loaded in BGR color space. Then, the BGR color format is interpreted and converted to RGB format. Next, we apply scaling to transform data so that it fits within a specific scale and

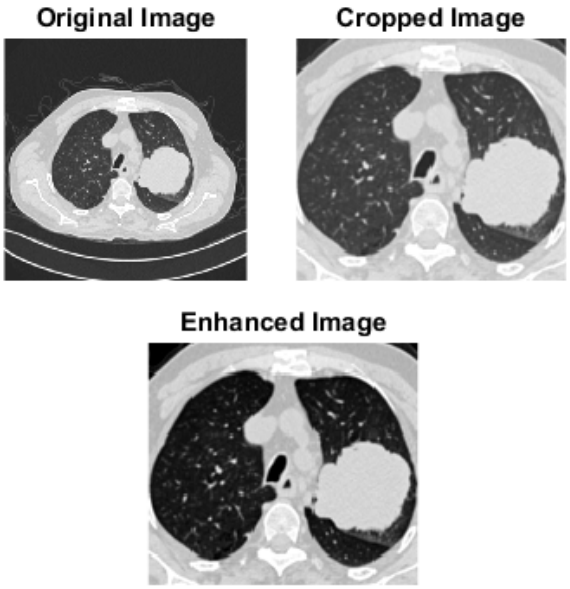

Fig. 3 Image enhancement

to change the range of data. The normalization is applied to change the observations so that they can be described as a normal distribution. We randomly shuffled the train pictures into a state of 25. Then we scale each pixel using a factor of 255. The majority of picture data has integer pixel values between 0 and 255. Small weight values are processed by neural networks, while high integer values might interfere with or slow down learning. Since, each pixel value of the image should range from 0 to 1, normalizing the pixel values is a good option. We use min-max scaling as follows to normalize the data such that the feature value remains within a specific range of 0 and 1.

$$x' = \frac{x - x_{min}}{x_{max} - x_{min}}, \tag{1}$$

where, x' is the normalized value. We divide all pixel values by 255, which is the biggest pixel value. Regardless of the actual range of pixel values that are present in the image, this is done across all channels.

3.2.2 Image cropping and enhancement

Method 2 of preprocessing is applied before applying the data for morphological feature extraction. It includes data loading, image resizing, cropping, and enhancement processes. First, all the collected CT scan images are loaded and converted to grayscale images. Then, the images are resized and cropped to get the required dimensions. Finally, the contrast level of the images is adjusted to enhance the image features such as boundaries and edges. The original image, the cropped image, and the enhanced image are shown in Figure 3. After applying the image cropping and enhancement process, the raw RGB image of 512×512×3 uint8 dimension is converted to a binary image of 136×151 logical dimension.

4 Feature Extraction

We propose the following two methods of feature extraction using transfer learning and morphological operations. The methods are explained in detail as follows.

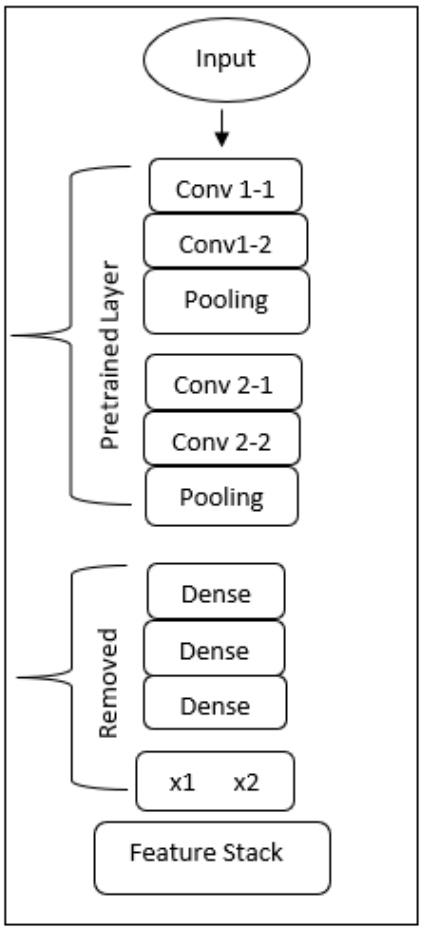

Fig. 4 VGG16 model for feature extraction

4.1 Transfer learning for Feature extraction

When a pre-trained model is repurposed for a different related task is known as transfer learning. As a deep Convolutional neural network (CNN) is difficult and expensive to train with small datasets and complex models. Since the transfer learning model can obtain improved accuracy with small datasets, we apply VGG16 [19] pre-trained model to implement transfer learning (TL) for feature extraction. VGG16 has an exceptional feature extraction capability, allowing us to utilize it in our research for feature extraction as it has a greater capacity to learn new features because it is deeper than certain transfer learning models, such as AlexNet. VGG16 uses just 3×3 convolution layers and 2×2 pooling layers repeatedly, which makes it significantly less complex than other transfer learning models like InceptionNet and enables it to generalize and adapt more effectively to a larger variety of data sets. VGG19 is a similar type of CNN model with 19 layers. However, due to the increased number of CNN layers of VGG19, the ability to fit complex functions also increases which, in turn, increases the training time significantly.

We use the VGG16 CNN architecture as shown in Figure 4 for TL feature extraction as it is deeper, less complex, and faster than other transfer learning models as VGG19, Inception V3, XCeption, and ResNet-50. VGG16 may be applied with data augmentation to prevent overfitting and improve accuracy. However, we apply VGG16 without data augmentation as it is faster than the method with data augmentation. We develop the TL feature extraction method in Python using the VGG16 model of 16 convolutional layers including the Maxpooling layers, 3 dense layers (2 fully connected layers and 1 SoftMax classifier), and an output layer of 1,000 nodes. Before TL feature extraction, the datasets are preprocessed using scaling and normalization. After applying

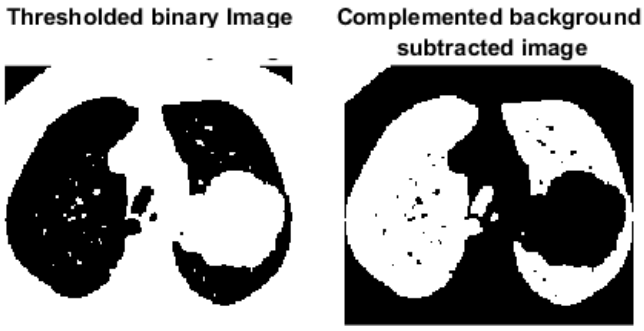

Fig. 5 ROI segmentation of the Malignant type tumor

feature extraction, a new dataset is created from the input image dataset of lung tumors using the pre-trained model. The detail steps are as follows.

1. First, the convolutional and pooling layers are imported and the fully-connected dense layers at the top of the model are removed.
2. Then, the image data are passed through the pre-trained layers to extract the visual features. Since the VGG16 model is trained on millions of photos, the convolutional layers can recognize the generic visual features of the images with the trained weights and provides a feature stack containing the recognized visual features.
3. The 3-dimensional feature stack is then flattened before applying it to other classifiers.

The extracted TL features are classified using other machine learning or deep learning classifiers.

4.2 Morphological Feature Extraction

Morphological feature extraction is developed in MATLAB. Image cropping and image enhancement are the preprocessing methods that are applied before morphological feature extraction. To extract the features, first image segmentation methods are applied to separate the region of interest (ROI) of the preprocessed CT images of the lung tumors. We use thresholding and morphological operations for ROI segmentation of the malignant, benign, and normal tumors. The ROI is required to be segmented to extract distinct features of different classes of tumors. Next, morphological features are extracted by measuring the geometrical properties of the segmented regions. The extracted features are then applied to the classifiers for classification. The methodologies are explained below.

4.2.1 Thresholding

Thresholding is the simplest method of image segmentation and a way to convert the gray-scale image to a binary image based on the computed threshold value. The threshold level indicates the intensity value of the image. There are several thresholding methods including the maximum entropy method, balanced histogram thresholding, Otsu's method (maximum variance), and k-means clustering. We apply Otsu's method [20] to compute the global threshold of the contrasted grayscale image. In the binary conversion, the output binary image replaces all pixels in the input grayscale with luminance greater than level with the value 1 (white) and replaces all other pixels with the value 0 (black). Figure 5 (left) shows the thresholded binary image of a malignant type tumor.

4.2.2 Morphological operations

We apply the following morphological operations on the thresholded binary images for the segmentation of the ROI of malignant, benign, and normal tumors and to remove unnecessary features.

1. Creating structuring element: First, we extract the background of the binary images by creating a morphological structuring element (SE) of disk shape.

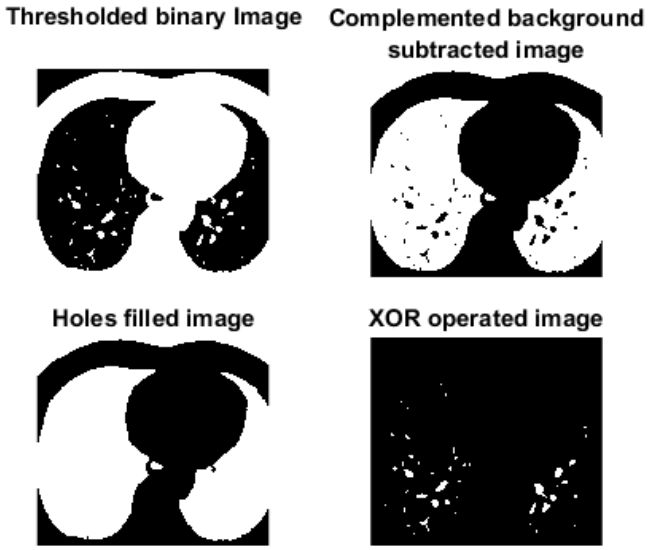

Fig. 6 ROI Segmentation of the Benign type tumor

2. Opening operation: Then we apply the morphological opening operation to open the SE from the binary image and to get the background of the image.
3. Background subtraction: The extracted background is then subtracted from the binary image to get the background subtracted image.
4. Complement image: The background-subtracted images are complemented. The complemented background subtracted binary image is considered as the ***ROI of the malignant*** type tumors.
5. Image fill operation: The image fill operation is applied to fill the holes in the complemented background subtracted binary images.
6. Logical XOR operation and complement: The logical exclusive OR operation is applied on the complemented images (step 4) and the holes-filled images (step 5) to obtain the ***ROI of the benign*** type tumors.
7. Complement the XOR-operated image: The XOR-operated image is complemented to get the ***ROI of the normal*** type tumors.

Figures 5, 6, and 7 show the different ROI segmentation processes of the malignant, benign, and normal-type tumors. Figure 5 (right) shows the complemented background subtracted ROI of a malignant type tumor and it is observed that the ROI segmentation of Malignant tumors includes steps 1 to 4 of the morphological operations. Figure 6 shows the thresholded binary image, the complemented background subtracted image, the holes-filled image, and the XOR-operated ROI of a benign type tumor and it is apparent that the ROI segmentation of Benign type tumors includes steps 1 to 6 of the morphological operations. Figure 7 shows the thresholded binary image, the complemented background subtracted image, the holes-filled image, and the complemented XOR-operated ROI of a normal type tumor. Thus, ROI segmentation of Normal type tumors includes all the proposed steps of morphological operations.

The system flow chart of the morphological feature extraction and classification is shown in Figure 8. Figure 8 illustrates the step-by-step morphological operations and the system flow of both the training and test phases. As we can see in Figure 8 that in the training phase, all the training images of the three types of tumors are gone through the morphological operations for ROI segmentation. However, in the test phase, morphological operations for malignancy are applied first and if malignancy is detected by the classifier, then no further morphological operations are applied for ROI segmentation of Benign or Normal type tumors. Similarly, if benign tumors are detected by the classifier then no further operations are applied for ROI segmentation of the Normal type tumors.

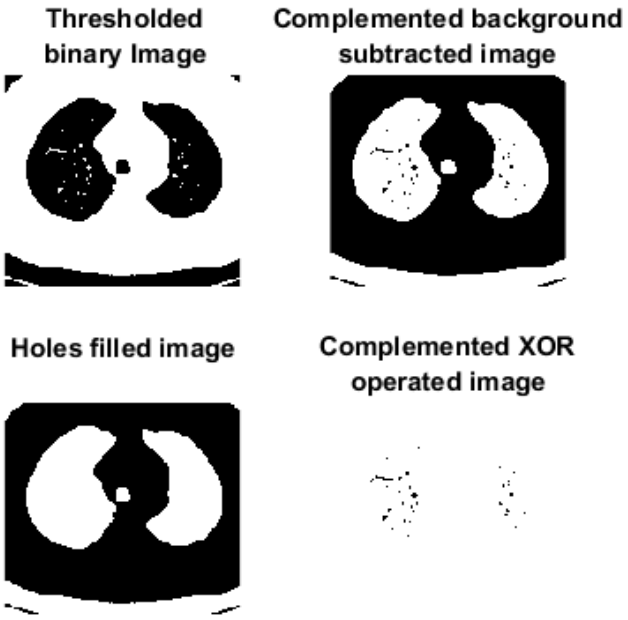

Fig. 7 ROI Segmentation of the Normal type tumor

4.2.3 Morphological feature extraction

In the morphological feature extraction module, the morphological features (MF) of the segmented ROI of the malignant, benign, or normal-type tumors are extracted by measuring the following four geometrical properties:

1. Area: It is a measure of the actual number of pixels in the region.
2. Eccentricity: Considering an ellipse having equivalent second-moments as the region, Eccentricity is measured as the ratio of the distance between the foci of the ellipse and the length of its major axis. This value is also referred to as the irregularity index of circularity or roundness. The value is between 0 and 1. An ellipse with 0 eccentricity can be defined as a circle and the ellipse can be defined as a line segment if the eccentricity is 1.
3. Perimeter: This is the distance around the boundary of the region which is measured by the number of pixels in the boundary of the region. The perimeter is calculated as

$$\text{Perimeter} = \sum_{i=}^{N-1} d_i \tag{2}$$

4. Compactness: Compactness is defined as the ratio of the area of an object to the area of a circle with the same perimeter. Benign tumors are more smooth and round in shape than malignant tumors. Therefore, we use the following alternate formula of compactness

$$\text{Compactness} = \frac{\text{Perimeter}^2}{2 \times \text{Area}} \tag{3}$$

By applying morphological feature extraction, the dimension of the extracted features is significantly reduced as compared to the dimension of the original raw data. The dimension of the extracted features is 4×1 double containing the four extracted features of each segmented region. The extracted morphological features are classified using machine learning and deep learning classifiers. As morphological feature extraction compresses the size of the training and test data significantly, it results in less computational complexity and reduced training and test time of classification.

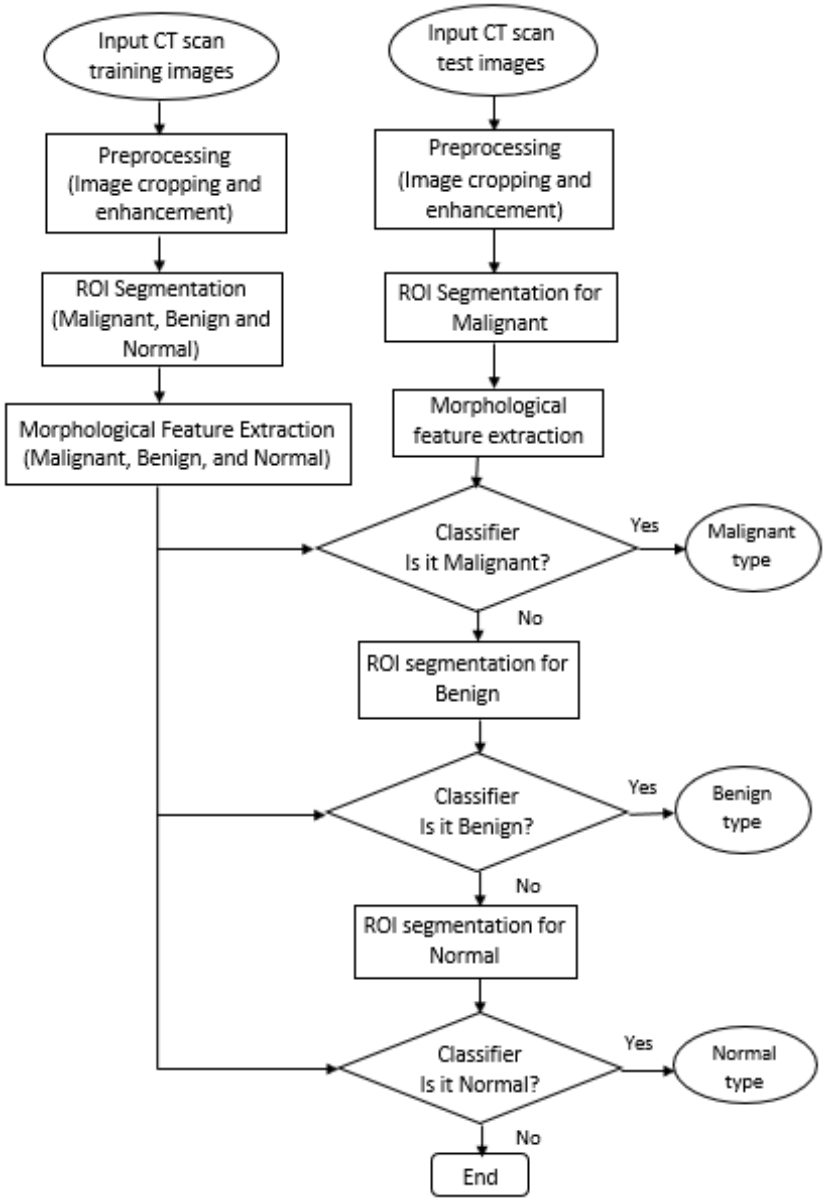

Fig. 8 Morphological feature extraction and classification flow chart

5 Classification

The preprocessed raw data or the extracted features of the lung tumors are applied to deep learning or machine learning-based classifiers for classification. The different types of classifiers are briefly explained below.

5.1 Deep learning classifier

The Convolutional Neural Network (CNN) architecture of the deep learning model as shown in Figure 9 is used for classification. Prior to deep learning, we add two convolutional layers with an input layer of (224, 224, 3) and an element-wise activation function on each of those, commonly known as a Rectified-Linear Unit (ReLu). The ability to activate the input nodes is decided by the ReLu layer. If the filters in the convolution layer pick up a visual characteristic, the activation is indicated. ReLu function operates by applying a max (0, x) function thresholded at 0. Followed by two Maxpooling

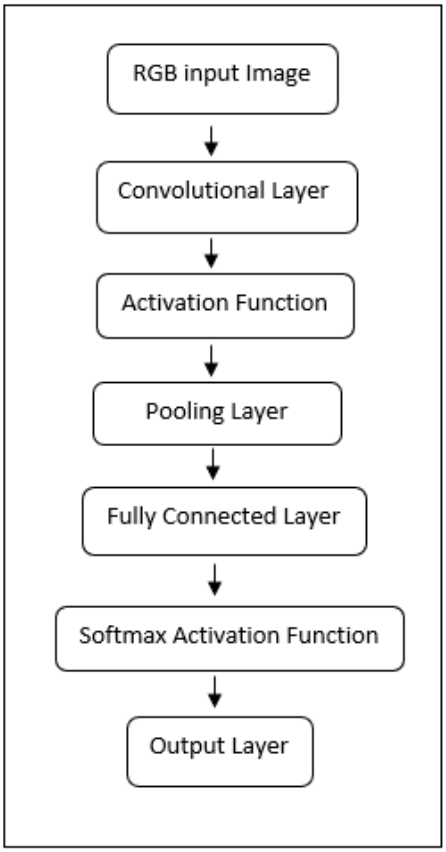

Fig. 9 Convolutional Neural Network Architecture

layers of (2, 2), a down-sampling strategy is applied to reduce the width and height of the output volume. After adding a flattened layer, two dense layers with 128 neurons and 3 neurons output, respectively are added. The model is then trained and tested using Google Colaboratory GPU. We chose the optimizer Adam and the sparse categorical cross-entropy loss function with batch size = 64, epoch = 20 for the compilation stage to optimize the model during training and to minimize the loss function.

5.2 Machine learning classifiers

In our proposed system, we apply the following supervised Machine Learning algorithms on preprocessed raw data, transfer-learning features, and on morphological features. In supervised machine learning, the model is trained to discover patterns in a dataset of features and labels and then used to predict the labels of features on a new dataset.

1. Decision Tree (DT): In the Decision Tree classification algorithm, internal nodes represent dataset attributes, branches represent decision rules and each leaf node provides the output of the decision in the tree-structured classifier [21].

2. k-Nearest Neighbors (KNN): The K-Nearest Neighbour method assumes that the new case and existing cases are similar and places the new case in the category that is most similar to the existing categories. The KNN method stores all available data and classifies a new data point based on its similarity to the existing data [22].

3. Random Forest (RF): Random forest is an ensemble learning method that operates by constructing a multitude of decision trees at training time. For classification tasks, the output of the random forest is the class selected by most trees. RF correct the decision trees' habit of overfitting to their training set [23].

4. Extra Trees (ET): The Extra Trees classifier, also known as Extremely Randomized Trees, is comparable to a Random Forest classifier [24]. We alter our approach to tree construction in order to add more variance to the ensemble. The following standards are used to build each decision stump:

i) Each stump is constructed using the training set's data.

ii) The best split is found by searching through a subset of randomly chosen features to construct the root node or any node (number of features). Each feature's split is determined randomly.

iii) The decision stump can go only as deep as one.

5. Extreme Gradient Boosting (XGB): Extreme Gradient Boosting (XGB) is a supervised, distributed, scalable gradient-boosted decision tree (GBDT) machine learning framework. For classification and regression, a GBDT is a decision tree ensemble learning approach similar to a random forest [25].

6. Support Vector Machine (SVM): Support Vector Machine classifier finds the optimum line or decision boundary for categorizing n-dimensional space into classes so that additional data points can be readily placed in the correct category. A hyperplane is the optimal choice boundary which is created by the support vectors [26].

7. Logistic Regression (LR): Logistic regression predicts a categorical dependent variable from a set of independent variables. It can generate probabilities and classify new data using both continuous and discrete datasets [27].

5.2.1 k-fold cross validation

The k-fold cross-validation is applied to split the datasets and to validate the test accuracy of all the datasets [28]. We apply 5-fold cross-validation where the datasets are shuffled to 42 random states and split into 5 groups each containing 20% of the total datasets. Then one of the groups is taken as the test dataset and the remaining groups are taken as the training dataset. Then the proposed model is fitted on the training datasets and evaluated on the test datasets. Finally, the evaluation score is recorded for each test group and averaged to evaluate the performance of the model.

6 Performance Evaluation

We apply the following performance metrics to evaluate the performance of the classification models [29].

6.1 Confusion matrix

Confusion Matrix is a visualization of ground-truth labels versus model predictions. Each row of the confusion matrix represents the instances in a predicted class and each column represents the instances in an actual class. Each cell in the confusion matrix represents any of the following evaluation factors:

1. True Positive (TP) signifies how many actual positive class samples are predicted correctly by the model.
2. True Negative (TN) signifies how many actual negative class samples are predicted correctly by the model.
3. False Positive (FP) signifies how many actual negative class samples are predicted incorrectly by the model.
4. False Negative (FN) signifies how many actual positive class samples are predicted incorrectly by the model.

6.2 Precision

Precision is the ability of a classifier not to label an instance positive that is actually negative. For each class, it is defined as the ratio of true positives to the sum of true and false positives.

$$\text{Precision} = \frac{TP}{TP + FP} \tag{4}$$

6.3 Recall

Recall is the ability of a classifier to find all positive instances. For each class, it is defined as the ratio of true positives to the sum of true positives and false negatives.

$$\text{Recall} = \frac{TP}{TP + FN} \tag{5}$$

6.4 F1 score

The F1 score is a weighted harmonic mean of precision and recall such that the best score is 1.0 and the worst is 0.0. Generally speaking, F1 scores are lower than accuracy measures as they embed precision and recall into their computation. As a rule of thumb, the weighted average of F1 should be used to compare classifier models, not global accuracy.

$$\text{F1 score} = \frac{2 \times \text{Recall} \times \text{Precision}}{(\text{Recall} + \text{Precision})} \tag{6}$$

6.5 Accuracy

Classification accuracy is defined as the number of correct predictions divided by the total number of predictions, multiplied by 100. The classification or test accuracy is calculated as

$$\text{Accuracy} = \frac{(TP + TN)}{(TP + FP + FN + TN)} \times 100 \tag{7}$$

6.6 Cross entropy loss function

In the classification model, the probability of each predicted class is compared to the desired output 0 or 1 of the actual class. A loss function is calculated based on the probability of how far it is from the actual expected value. The penalty is logarithmic resulted in a large score for large differences close to 1 and small score for small differences tending to 0. Cross-entropy loss is used to optimize the model by adjusting the weights during training to minimize the loss tends to 0. The Cross-entropy loss function is defined as [30]

$$L_{CE} = -\sum_{i=1}^{n} t_i log(p_i), \quad \text{for n classes} \tag{8}$$

where, n is the number of classes, t_i is the true label and p_i is the Softmax probability for the i^{th} class.

7 Experimentation and Results

We collect a dataset of 1097 CT scan images of three types of lung tumors in jpg format from the Kaggle database [18]. The database contains an assortment of Computed Tomography (CT) images of patients with and without lung diseases. The dataset contains 120 CT scan images of the benign class, 561 of the malignant class, and 416 of the normal class. The proportion of each class of data is given in Figure 10. To develop the lung tumor detection and classification system, 80% of the

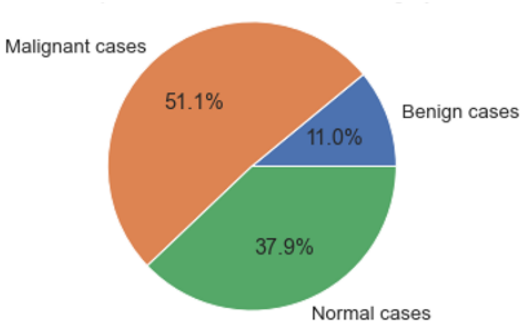

Fig. 10 Proportion of different classes of lung tumor images

Table 1 Data Splitting

Classes	Train	Test
Benign	96	24
Malignant	448	113
Normal	332	84

Table 2 Accuracy score of CNN with preprocessed dataset and the TL features

Evaluation Parameters	Preprocessed data	TL features
Training Accuracy	100.00%	100.00%
Test Accuracy	98.64%	95.928%
Training Loss	0.0001	0.00079
Test Loss	0.053	0.103
Precision	0.987	0.962
Recall	0.986	0.959
F1 Score	0.986	0.960

dataset is trained with the known label of different types of tumors and 20% of the dataset is tested. The data are split into training and test data as shown in Table 1.

We simulate the proposed transfer learning for feature extraction and classification methods based on deep learning and machine learning in Python using various popular data analysis tools and libraries. The libraries include pandas, scipy.io, numpy, matplotlib, seaborn. The classifiers are developed using the Keras, TensorFlow, and Scikit-Learn tools. The morphological feature extraction methods are developed in MATLAB. The computational environment of simulation, training and testing of the proposed system is based on a 64-bit Windows operating system with an x64-based Intel(R) Core(TM) i7-5500U CPU with 2.40 GHz processor and 8.00 GB of installed RAM. In addition, we leverage the NVIDIA GeForce 840M GPU for efficient computation.

First, the CT image datasets are preprocessed using our proposed methods for resizing, smoothing, and enhancement in MATLAB. The results of the preprocessing methods are shown in Figure 3. Then, we apply the proposed deep learning Convolutional Neural Network (CNN) on the preprocessed raw dataset and the extracted TL features to classify the lung tumors. Table 2 summarizes the accuracy scores of the deep learning CNN-based classification approach using preprocessed data. We also analyze the training and test accuracy of the deep CNN classifier for an increasing number of epochs. Figures 11 and 12 show the accuracy curve and the loss curve of CNN for an increasing number of epochs using preprocessed datasets. It is observed in Figure 11 that both training and test accuracy improves with the increasing number of epochs. Figure 12 shows that both the training and test loss decrease with the increasing number of epochs. It is also observed from Table 2 and Figure 11 that CNN obtains 98.64% test accuracy using preprocessed raw data. We also apply machine learning-based classification algorithms to the preprocessed raw data. Table 3 shows the

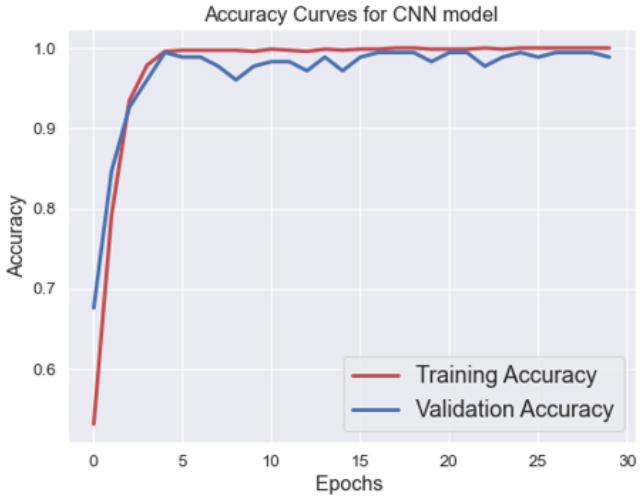

Fig. 11 Accuracy Curve

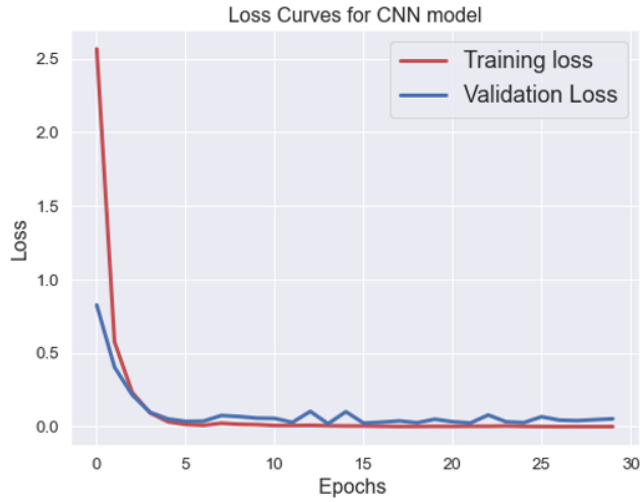

Fig. 12 Loss curve

Table 3 Evaluation Score of Machine learning algorithms with preprocessed raw dataset

Algorithm	Precision	Recall	F1 score	Accuracy
DT	0.876	0.869	0.871	86.88%
KNN	0.969	0.968	0.967	96.83%
RF	0.958	0.955	0.951	95.48%
ET	0.991	0.991	0.991	99.09%
XGB	0.996	0.995	0.995	99.55%
SVM	0.965	0.964	0.963	96.38%
LR	1.000	1.000	1.000	100%

accuracy scores using different machine learning algorithms with preprocessed raw datasets. The highest accuracy of 100% is observed using logistic regression (LR).

Then, for high-speed data processing, we apply feature extraction methods to reduce the dimensionality of raw data. First, we apply transfer learning for feature extraction using VGG16 CNN model. The extracted TL features are classified using deep learning and machine learning methods. The performance scores using deep learning CNN classification on the extracted TL features are

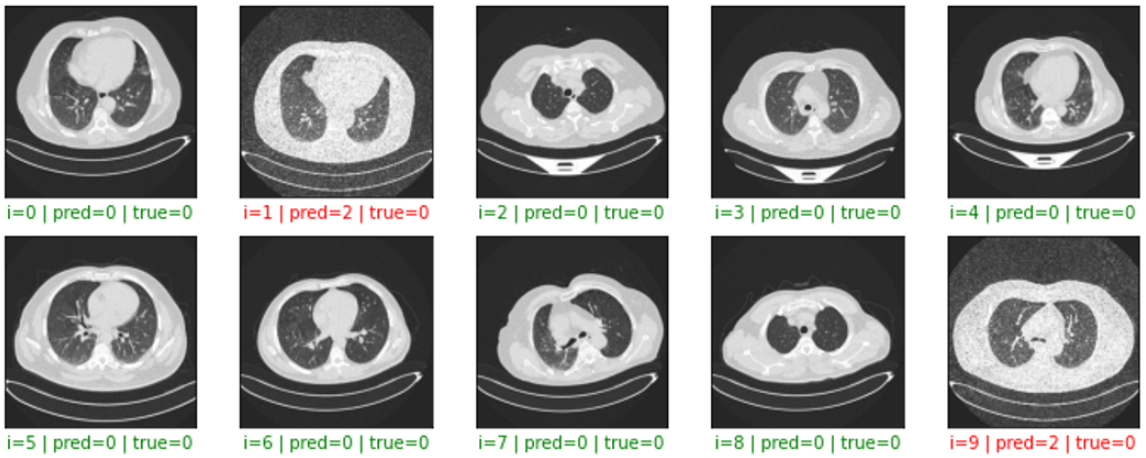

Fig. 13 Few of the predicted results using CNN

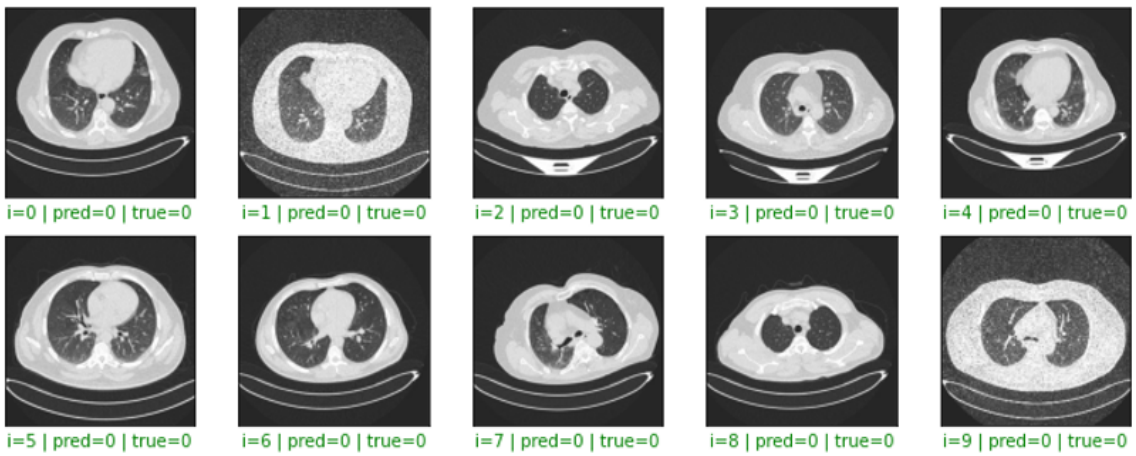

Fig. 14 Few of the predicted results using Logistic regression

Table 4 Evaluation Score of machine learning algorithms on the Transfer learning features

Algorithm	Precision	Recall	F1 score	Accuracy
DT	0.969	0.968	0.969	96.83%
KNN	0.969	0.968	0.967	96.83%
RF	0.987	0.986	0.986	98.64%
ET	0.991	0.991	0.991	99.09%
XGB	0.996	0.995	0.995	99.55%
SVM	0.971	0.968	0.966	96.83%
LR	1.000	1.000	1.000	100%

included in Table 2 which shows that 95.928% accuracy is obtained using the TL features. A few of the predicted results including two false predictions of CNN using raw data are shown in Figure 13. Here, "true" indicates the real label and "pred" indicates the predicted label. We can see that two false predictions indexed as i=1 and i=9 detect benign tumors as normal. Table 4 shows the accuracy scores using different machine learning algorithms with TL features. As we can see among all machine learning algorithms, the logistic regression (LR) shows 100% accuracy using the extracted TL features. Significantly high accuracy is also observed using *ET* and *XGB* classifiers. Figure 14 shows a few prediction results using logistic regression (LR).

Table 5 Evaluation Score of Machine learning algorithms on the Morphological features

Algorithm	Precision	Recall	F1 score	Accuracy
DT	0.986	0.985	0.985	98.49%
KNN	0.996	0.996	0.996	99.56%
RF	0.996	0.996	0.996	99.56%
ET	0.996	0.996	0.996	99.56%
XGB	0.996	0.996	0.996	99.56%
SVM	0.996	0.996	0.996	99.6%
LR	0.989	0.989	0.989	98.93%

Table 6 Comparison of classification accuracy using different machine learning algorithms

Algorithm	Preprocessed data	TL features	Morphological features
DT	86.878%	96.833%	98.49%
KNN	96.833%	96.833%	99.56%
RF	95.475%	98.643%	99.56%
ET	99.095%	99.095%	99.56%
XGB	99.548%	99.548%	99.56%
SVM	99.380%	96.833%	99.6%
LR	100%	100%	98.93%

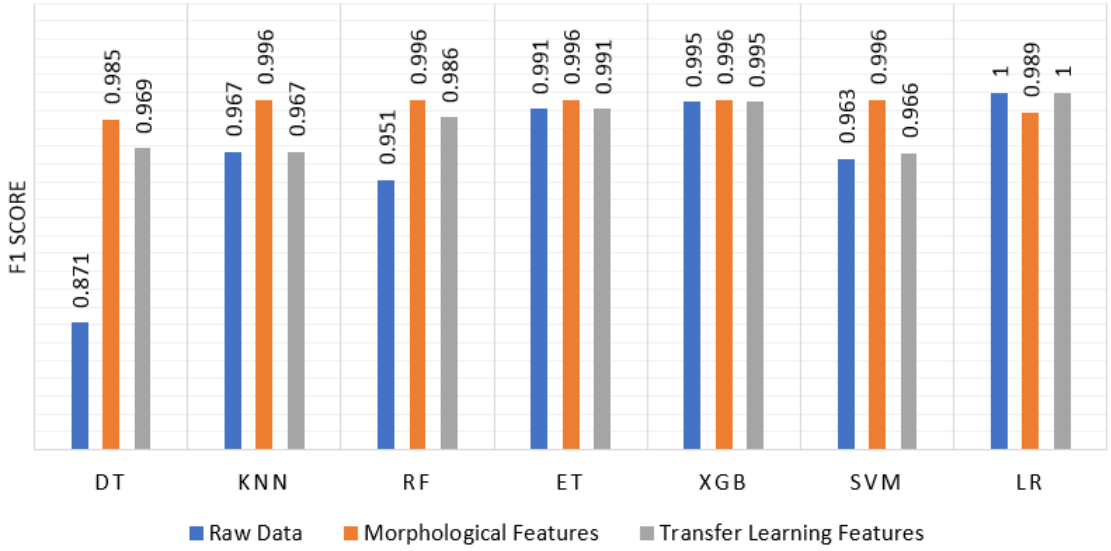

Fig. 15 Comparison of the F1 score using different proposed methods

Then, the proposed morphological segmentation and feature extraction is applied on the preprocessed data to further improve computational intelligence by reducing computational complexity. The results of the morphological segmentation of the ROI of malignant, benign, and normal tumors are shown in Figures 5, 6, and 7, respectively. The extracted features of the segmented ROI are then applied to the machine learning algorithms for classification. The accuracy scores of the machine learning approaches on the extracted morphological features are included in Table 5. As we can see in Table 5 that all of the machine learning algorithms show significantly high accuracy using the morphological features. Most of the classifiers including KNN, RF, ET, XGB show 99.56% accuracy whereas the best accuracy of 99.6% is observed using the SVM classifier.

Table 6 compares the achievable accuracy of all the proposed classification models using machine learning. Figure 15 compares the obtained F1 score of all machine learning classification algorithms using raw data, morphological features, and transfer learning features. As we can see in Table 6 that

Table 7 Training time comparison of all machine learning algorithms

Algorithm	**Preprocessed data** (sec)	**TL features** (sec)	**Morphological features** (sec)
DT	64.642	20.476	0.011
KNN	0.19	0.146	0.014
RF	10.973	4.955	0.339
ET	8.132	6.217	0.236
XGB	617.49	300.629	0.806
SVM	73.834	44.826	0.032
LR	49.486	37.519	0.333

100% accuracy is achieved by logistic regression (LR) using both raw data and TL features. It is also observed in Table 6 and Figure 15 that with the extracted low dimensional (4×1) morphological features, all the machine learning algorithms perform equally well with high accuracy and F1 score. Among those, SVM shows the best accuracy of 99.6%.

Table 7 shows the training time (in seconds) comparison for all the machine learning classification algorithms. Here, we can see that the preprocessed raw data requires a high processing time for training among which the XGB requires the highest training time of 617.49 *sec*. It is also observed in Table 7 that the training time is reduced slightly by applying transfer learning-based feature extraction. However, the morphological feature extraction reduces the training time significantly for all the classification algorithms by extracting the low dimensional features.

Figure 16 shows the multi-class confusion matrix of 4 (four) of the proposed CNN-deep learning and machine learning (ML) methods using preprocessed raw data and the extracted features. In the confusion matrices, X-axis indicates the actual value and Y-axis indicates the predicted value. The confusion matrix of CNN using the preprocessed raw data is shown in Figure 16(a) where we can see that 2 of the actual benign cases are predicted as normal and 1 of the actual normal cases is predicted as malignant during classification. That means 2 FN for the Benign class, 1 FP for the Malignant class, 2 FP for the Normal class, and 1 FN for the Normal class. It is also observed that there are 22 true positives (TP) for Benign, 113 TP for Malignant, and 83 TP for Normal classes. The performance evaluation scores are calculated by putting the TP, FP, TN, and FN values of the confusion matrices in eqs. (4)-(7). The calculated evaluation scores of CNN using raw data are included in Table 2. Similarly, Figures 16(b) and 16(c) show the confusion matrix of the LR approach with raw data and TL features, respectively where we can see that the lung tumors of all the cases are classified correctly without any false predictions. Figure 16(d) shows the confusion matrix using SVM with morphological features where it can be observed that 1 of the actual malignant cases is predicted as normal during classification, i.e., 1 FN for the Malignant class and 1 FP for the Normal class. In this way, all the performance evaluation scores are calculated using the evaluation factors (TP, TN, FP, FN) from the confusion matrix for all the proposed algorithms and are included in Tables 2, 3, 4 and 5, respectively. It is observed that all the reported performance evaluation scores agree with the confusion matrix.

Tables 6 and 7 present the comparative results of the seven ML algorithms using the preprocessed raw data, transfer learning (TL) features, and morphological features. It is observed that LR performs the best with preprocessed data and TL features. Whereas, using the low dimensional morphological features, all the ML algorithms perform with reasonably high accuracy among which KNN and SVM perform the best with the least computational time. Therefore, 5-fold cross-validation is applied to mitigate overfitting problems and to verify the best possible accuracy using the LR, KNN, and SVM algorithms. The cross-validation results are presented in Table 8. It is observed in Table 8 that LR performs with 99.36% and 99.27% accuracy with preprocessed data and TL features in 23.71 sec and 16.51 sec computational time, respectively. Whereas, both KNN and SVM perform with 99.76% accuracy in 0.017 sec and 0.008 sec time, respectively. Thus, it may be concluded that using the low dimensional morphological features, KNN and SVM classification algorithms perform the best in the least computational time. Table 9 compares the accuracy of the proposed works to other related

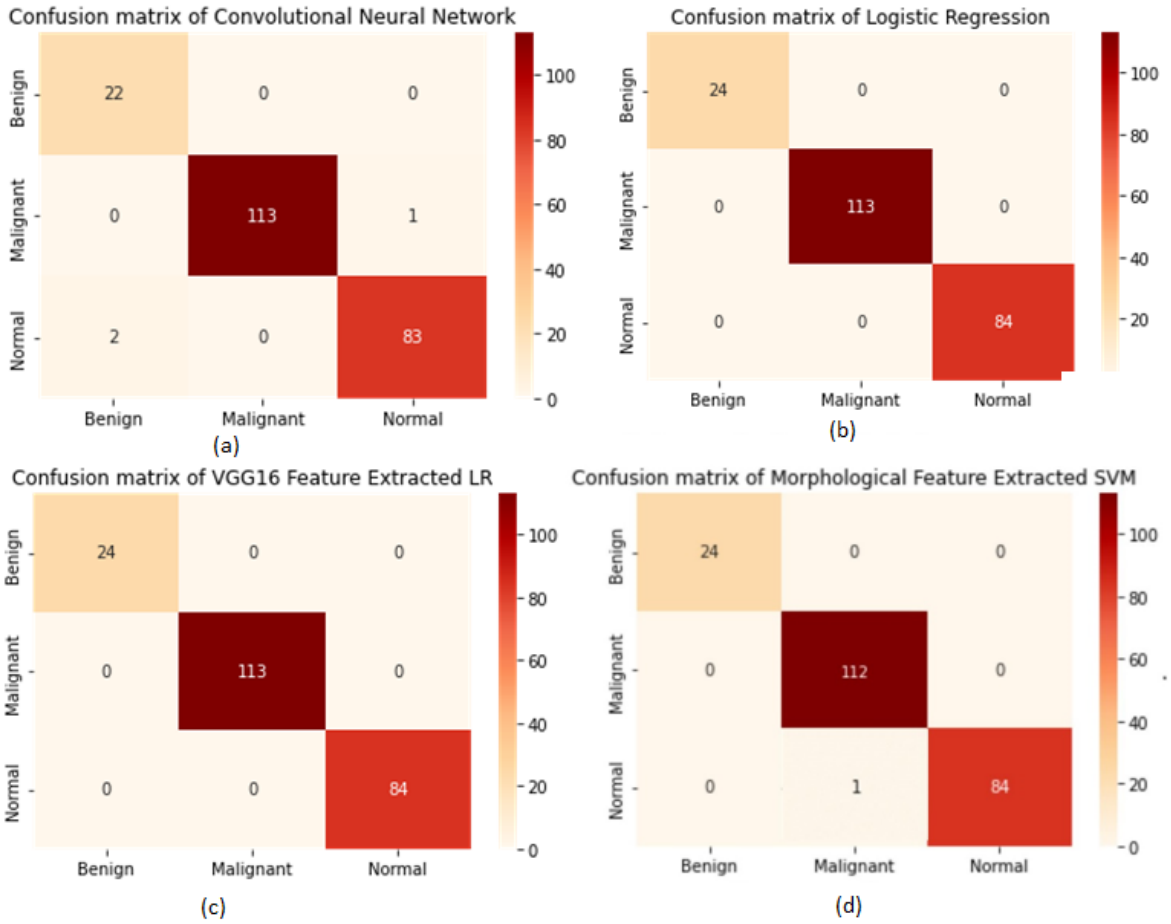

Fig. 16 (a) Confusion matrix of CNN using raw data, (b) Confusion matrix of LR using raw data, (c) Confusion matrix of LR using Tranfer learning features, (d) Confusion matrix of SVM using Morphological features.

Table 8 Best possible accuracy and computational time using 5-fold cross-validation

Data	ML Algorithms	Accuracy	Time
Preprocessed data	LR	99.36%	23.71 sec
TL features	LR	99.27%	16.51 sec
Morphological features	KNN	99.76%	0.017 sec
Morphological features	SVM	99.76%	0.008 sec

works in the literature. It is apparent from the comparison that the proposed works outperform the literature with high computational intelligence and accuracy.

8 Conclusion

Early detection and classification of lung tumors are required to increase the survival rate of the patients. Thus, a system is required with high computational intelligence and low complexity. In this paper, we have proposed lung tumor detection and classification using different preprocessing steps, ROI segmentation, feature extraction, and classification methods. First, we have applied different deep learning and machine learning-based classification algorithms to the preprocessed raw CT scan data. It is observed that using the deep learning-based CNN model, 98.64% accuracy is acquired and using machine learning-based logistic regression (LR), 100% accuracy is acquired with the preprocessed raw dataset. However, since preprocessed raw data requires a high processing time, we have

Table 9 Accuracy comparison to other related works

Algorithms	**Data**	**Segmentation and Feature extraction**	**Classifier**	**Binary/ Multi-class**	**Cross-validation**	**Accuracy**	**Training time** (s)
Günaydin et al [5] 2019	JSRT CT images	-	ANN and Decision Trees (DT)	Binary	No	82.43% 93.24%	-
Punitha-vathy et al [6] 2019	PET/CT images	3 Texture and 10 fractal features	SVM with RBF kernel	Binary	Yes	98.10%	-
Tao et al [7] 2020	CT images	DenseNet	DenseNet-NSCR	Binary	Yes	99.10%	3234.63
Moitra et al [10] 2020	LIDC-IDRI PET/CT images	Image segmentation and 33 MSER-SURF features	1D CNN	Binary	No	96 ± 3%	-
Boban et al [11] 2020	CT images	Gray level Co-occurance Matrix (GLCM) of 8 features	MLP, SVM, KNN	Multi	No	98%, 70.45% 99.2%	-
Abdullah et al [12] 2021	UCI ML dataset	-	SVM, KNN, CNN	Multi	Yes	95.56%, 92.11%, 88.40%	1.77 0.01 3.79
Nanglia et al [14] 2021	CT images	SURF and Generic algorithm (GA)	SVM with FFBPNN	Binary	No	98.08%	-
Kareem et al [15] 2021	IQ-OTH/ NCCD CT images	Gabor and GLCM features	SVM	Binary	No	89.88%	-
Pandian et al [17] 2022	CT images	Google net	CNN	Binary	No	98%	-
Proposed	IQ-OTH/ NCCD CT images	-	CNN	Multi	No	98.64%	-
Proposed	IQ-OTH/ NCCD CT images	TL VGG16	CNN	Multi	No	95.92%	-
Proposed	IQ-OTH/ NCCD CT images	-	LR	Multi	No	99.36%	23.71
Proposed	IQ-OTH/ NCCD CT images	VGG16 TL	LR	Multi	No	99.27%	16.51
Proposed	IQ-OTH/ NCCD CT images	Morphological segmentation and feature extraction	KNN SVM	Multi	Yes	99.76% 99.76%	0.017 0.008

applied two feature extraction methods to extract low-dimensional features to reduce the processing time. First, we have applied the VGG16 model to extract transfer learning (TL) features of the preprocessed data. Hence, we have obtained 95.928% accuracy using deep learning CNN and 100% accuracy using the LR method with the extracted TL features with a comparatively low processing time of training. Then, to further improve the computational intelligence, we have proposed morphological segmentation and feature extraction to extract low-dimensional features. The extracted morphological features are applied for classification using machine learning algorithms. It is observed that all the machine learning algorithms show significantly high classification accuracy with reduced training time using the low dimensional morphological features. Then, 5-fold cross-validation methods is applied to mitigate the overfitting problem. It is observed that LR performed with 99.36% and 99.27% accuracy using preprocessed data and TL features in 23.71 sec and 16.51 sec computational time, respectively. Whereas, both KNN and SVM performed with 99.76% accuracy in 0.017 sec and 0.008 sec time, respectively. Thus, it may be concluded that a significantly high accuracy of lung tumor detection and classification is possible to be achieved with the machine learning algorithms applied on the extracted low dimensional morphological features with low computational complexity and time. Therefore, the proposed methods recommend extracting low-dimensional morphological features and choosing machine learning-based classifiers for real-time lung cancer recognition.

Declarations

Ethical Approval

We have used lung cancer datasets collected in the Iraq-Oncology Teaching Hospital/National Center for Cancer Diseases (IQ-OTH/NCCD) over a period of three months. It includes CT scans of patients diagnosed with lung cancer in different stages, as well as healthy subjects. The IQ-OTH/NCCD slides were marked by oncologists and radiologists. The source of the collected IQ-OTH/NCCD lung cancer dataset has been cited in this paper.

Availability of supporting data

The IQ-OTH/NCCD Lung Cancer Dataset are available at the Mendeley Data repository and the Kaggle data archive.

Competing interests

The authors declare no conflict of interest.

Funding

No funding was received for this manuscript.

Authors' contributions

1. Nafe Muhtasim Hye - developed the deep learning CNN architecture, and the transfer learning VGG16 model, applied preprocessing, deep learning, and machine learning classifiers, and prepared Figures 4, 9, and 10-16.
2. Umma Hany - developed the morphological segmentation and feature extraction, applied preprocessing and machine learning classifier, contributed to the literature review, prepared Figures 1-3, and 5-8, and wrote the main manuscript.
3. Tahmina Islam- wrote the "Machine learning classifiers" subsection and the "Performance Evaluation" section, contributed to the literature review, and reviewed the manuscript.
4. Nusrat Nawreen - developed five morphological operations in Matlab, and contributed to the literature review.
5. Abdullah Al Mamun - collected datasets from Kaggle and reviewed the manuscript.

Acknowledgements

We thank the contributor of the dataset available at the Mendeley Data repository and the IQ-OTHNCCD lung cancer dataset archive of Kaggle. We also thank the Department of Electrical and Electronic Engineering, Ahsanullah University of Science and Technology for providing the necessary resources to conduct the research.

References

[1] P. Radhika, R. A. Nair, and G. Veena, "A comparative study of lung cancer detection using machine learning algorithms," in *IEEE International Conference on Electrical, Computer and Communication Technologies*. IEEE, 2019, pp. 1–4.

[2] "Differences between a malignant and benign tumor," [Online accessed 2022-04-17], http://www.differencebetween.net/science /health/difference-between-benign-and-malignant/.

[3] C. Kaushal, S. Bhat, D. Koundal, and A. Singla, "Recent trends in computer assisted diagnosis (CAD) system for breast cancer diagnosis using histopathological images," *Irbm, Elsevier*, vol. 40, no. 4, pp. 211–227, 2019.

[4] P. Chaturvedi, A. Jhamb, M. Vanani, and V. Nemade, "Prediction and classification of lung cancer using machine learning techniques," in *IOP Conference Series: Materials Science and Engineering*, vol. 1099, no. 1. IOP Publishing, 2021, p. 012059.

[5] Ö. Günaydin, M. Günay, and Ö. Şengel, "Comparison of lung cancer detection algorithms," in *Scientific Meeting on Electrical-Electronics & Biomedical Engineering and Computer Science*. IEEE, 2019, pp. 1–4.

[6] K. Punithavathy, S. Poobal, and M. Ramya, "Performance evaluation of machine learning techniques in lung cancer classification from PET/CT images," *FME Transactions*, vol. 47, no. 3, pp. 418–423, 2019.

[7] Z. Tao, H. Bingqiang, L. Huiling, Y. Zaoli, and S. Hongbin, "NSCR-based DenseNet for lung tumor recognition using chest CT image," *BioMed Research International, Hindawi*, vol. 2020, 2020.

[8] K. Pradhan and P. Chawla, "Medical internet of things using machine learning algorithms for lung cancer detection," *Journal of Management Analytics, Taylor & Francis*, vol. 7, no. 4, pp. 591–623, 2020.

[9] H. Hu, Q. Li, Y. Zhao, and Y. Zhang, "Parallel deep learning algorithms with hybrid attention mechanism for image segmentation of lung tumors," *IEEE Transactions on Industrial Informatics*, vol. 17, no. 4, pp. 2880–2889, 2020.

[10] D. Moitra and R. K. Mandal, "Classification of non-small cell lung cancer using one-dimensional convolutional neural network," *Expert Systems with Applications, Elsevier*, vol. 159, p. 113564, 2020.

[11] B. M. Boban and R. K. Megalingam, "Lung diseases classification based on machine learning algorithms and performance evaluation," in *International Conference on Communication and Signal Processing*. IEEE, 2020, pp. 0315–0320.

[12] D. M. Abdullah, A. M. Abdulazeez, and A. B. Sallow, "Lung cancer prediction and classification based on correlation selection method using machine learning techniques," *Qubahan Academic Journal*, vol. 1, no. 2, pp. 141–149, 2021.

[13] N. Nawreen, U. Hany, and T. Islam, "Lung cancer detection and classification using ct scan image processing," in *International Conference on Automation, Control and Mechatronics for Industry (ACMI)*. IEEE, 2021, pp. 1–6.

[14] P. Nanglia, S. Kumar, A. N. Mahajan, P. Singh, and D. Rathee, "A hybrid algorithm for lung cancer classification using SVM and Neural Networks," *ICT Express, Elsevier*, vol. 7, no. 3, pp. 335–341, 2021.

[15] H. F. Kareem, M. S. Al-Huseiny, F. Y. Mohsen, and K. Al-Yasriy, "Evaluation of svm performance in the detection of lung cancer in marked ct scan dataset," *Indonesian Journal of Electrical Engineering and Computer Science*, vol. 21, no. 3, p. 1731, 2021.

[16] H. Alyasriy and A. Muayed, "The IQ-OTHNCCD Lung Cancer Dataset," *Mendeley Data*, vol. 1, p. 2020, 2021.

[17] R. Pandian, V. Vedanarayanan, D. R. Kumar, and R. Rajakumar, "Detection and classification of lung cancer using CNN and Google net," *Measurement: Sensors*, vol. 24, p. 100588, 2022.

[18] "The IQ-OTHNCCD Lung Cancer Dataset," https://www.kaggle.com/datasets/antonixx/the-iqothnccd-lung-cancer-dataset, [Online accessed 2022-04-19].

[19] M. James, "Hands-on Transfer Learning with Keras and the VGG16 Model," https://www.learndatasci.com/tutorials/hands-on-transfer-learning-keras/, [Online accessed 2022-07-20].

[20] N. Otsu, "A threshold selection method from gray-level histograms," *IEEE transactions on systems, man, and cybernetics*, vol. 9, no. 1, pp. 62–66, 1979.

[21] L. Rokach and O. Maimon, "Decision trees," in *Data mining and knowledge discovery handbook*. Springer, 2005, pp. 165–192.

[22] G. Guo, H. Wang, D. Bell, Y. Bi, and K. Greer, "KNN model-based approach in classification," in *OTM Confederated International Conferences" On the Move to Meaningful Internet Systems"*. Springer, 2003, pp. 986–996.

[23] L. Breiman, "Random forests," *Machine learning, Springer*, vol. 45, no. 1, pp. 5–32, 2001.

[24] P. Geurts, D. Ernst, and L. Wehenkel, "Extremely randomized trees," *Machine learning, Springer*, vol. 63, no. 1, pp. 3–42, 2006.

[25] T. Chen and C. Guestrin, "Xgboost: A scalable tree boosting system," in *ACM SIGKDD international conference on knowledge discovery and data mining*, 2016, pp. 785–794.

[26] Y. Zhang, "Support vector machine classification algorithm and its application," in *International conference on information computing and applications*. Springer, 2012, pp. 179–186.

[27] R. E. Wright, "Logistic regression." *American Psychological Association*, 1995.

[28] J. Brownlee, "A Gentle Introduction to k-fold Cross-Validation," *in Statistics, https://machinelearningmastery.com/k-fold-cross-validation/*, [2023-10-04].

[29] B. Aayush, "Performance Metrics in Machine Learning [Complete Guide]," https://neptune.ai/blog/performance-metrics-in-machine-learning-complete-guide, [Online accessed 2022-07-21].

[30] W. Rose, "Cross-Entropy Loss and Its Applications in Deep Learning," https://neptune.ai/blog/cross-entropy-loss-and-its-applications-in-deep-learning, [Online accessed 2022-09-02].